

Experimental Realization of Optimal Noise Estimation for a General Pauli Channel

A. Chiuri,¹ V. Rosati,¹ G. Vallone,^{1,2} S. Pádúa,³ H. Imai,⁴ S. Giacomini,¹ C. Macchiavello,⁴ and P. Mataloni^{1,5}

¹*Dipartimento di Fisica, Sapienza Università di Roma, Piazzale Aldo Moro 5, I-00185 Roma, Italy*

²*Department of Information Engineering, University of Padova, I-35131 Padova, Italy*

³*Departamento de Física, Universidade Federal de Minas Gerais. Caixa Postal 702, Belo Horizonte, MG 30123-970, Brazil*

⁴*Dipartimento di Fisica "A. Volta" and INFN-Sezione di Pavia, via Bassi 6, 27100 Pavia, Italy*

⁵*Istituto Nazionale di Ottica (INO-CNR), L.go E. Fermi 6, I-50125 Firenze, Italy*

(Dated: November 10, 2022)

We present the experimental realization of the optimal estimation protocol for a Pauli noisy channel. The method is based on the generation of 2-qubit Bell states and the introduction of quantum noise in a controlled way on one of the state subsystems. The efficiency of the optimal estimation, achieved by a Bell measurement, is shown to outperform quantum process tomography.

PACS numbers: 42.50.Dv, 03.67.Bg, 42.50.Ex

Introduction.- Quantum noise is unavoidably present in any realistic implementation of quantum tasks, ranging from quantum communication protocols [1] to quantum information processing devices and quantum metrology [2, 3]. It is therefore of great interest to develop experimental methods to estimate the level of noise in the system under consideration. Quantum Process Tomography (QPT) [4], which has already been implemented in various experimental realizations [5, 6], represents a well-known method to identify an unknown noise. In many realistic scenarios, however, some *a priori* information on the kind of noise is known and therefore the problem of measuring it is equivalent to estimate few noise parameters in the most efficient way. This is the context of quantum channel estimation [7].

A quantum channel estimation problem is formulated as follows. We need to estimate the true value of the d -dimensional parameter θ for a given smooth parametric family $\{\Gamma_\theta; \theta \in \Theta \subset \mathbb{R}^d\}$ of quantum channels. The estimation scheme is twofold: first we input a well-prepared quantum state described by the density operator τ to Γ_θ , then we perform a quantum state estimation on the statistical model $\{\Gamma_\theta(\tau)\}_\theta$. Thus, the problem is to seek an optimal input τ for the channel and an optimal quantum state estimation on the model $\{\Gamma_\theta(\tau)\}_\theta$. A quantum estimator is a pair $(\check{\theta}, M)$ of a positive-operator valued measure (POVM) M taking values on an outcome set Ξ and an estimating function $\check{\theta} : \Xi \rightarrow \Theta$. Once a POVM M is fixed, the problem is reduced to the classical parameter estimation of densities $P_\theta^M(dx) = \text{Tr} \Gamma_\theta(\tau) M(dx)$ of outcome probabilities. The aim is then to find an input state τ and a quantum estimator $(\check{\theta}, M)$ which minimizes the covariance matrix:

$$\mathbb{V}_\theta[\check{\theta}, M]^{ij} = \mathbb{E}_\theta[(\check{\theta}^i - \theta^i)(\check{\theta}^j - \theta^j)] \quad (1)$$

where $i, j = 1, \dots, d$ and \mathbb{E}_θ denotes the expectation with respect to P_θ^M .

In this work we present an experimental implementation of an optimal quantum channel estimation scheme for a qubit Pauli channel. The action of such a family of channels on the

density operator ρ of a qubit can be described as [4]

$$\Gamma_{\{p\}}[\rho] = \sum_{i=0}^3 p_i \sigma_i \rho \sigma_i \quad (2)$$

where σ_0 is the identity operator, $\{\sigma_i\}$ ($i = 1, 2, 3$) are the three Pauli operators $\sigma_x, \sigma_y, \sigma_z$ respectively, and $\{p_i\}$ represent the corresponding probabilities ($\sum_{i=0}^3 p_i = 1$).

The optimal channel estimation scheme is achieved as follows [8]. The optimal input state is represented by a Bell state for two qubits, for example the singlet state $|\psi^-\rangle = \frac{1}{\sqrt{2}}(|01\rangle - |10\rangle)$, where only one of the qubits is affected by the noisy channel while the other one is left untouched. The optimal measurement consists of a Bell measurement on the two qubits at the channel output, namely the projective measurement $M = \{|\psi^-\rangle\langle\psi^-|, |\psi^+\rangle\langle\psi^+|, |\phi^-\rangle\langle\phi^-|, |\phi^+\rangle\langle\phi^+|\}$. The outcome probabilities then provide an optimal estimation of the channel parameters p_i .

As mentioned above, this scheme is optimized by minimizing the covariance matrix of the estimation error (1). According to the quantum Cramér-Rao theorem [9], the minimum covariance matrix in this case is given by [8]

$$\mathbb{V}_p[\varepsilon] = J_p^{-1}[\varepsilon] = \begin{bmatrix} p_1(1-p_1) & -p_2p_1 & -p_3p_1 \\ -p_1p_2 & p_2(1-p_2) & -p_3p_2 \\ -p_1p_3 & -p_2p_3 & p_3(1-p_3) \end{bmatrix} \quad (3)$$

where $J_p^{-1}[\rho]$ is the quantum Fisher information matrix [9] of the output state ρ .

The experimental implementation of this optimal estimation scheme is based on a quantum optical setup, where the state of the two qubits is represented by polarization states of two photons and the action of the Pauli channel is introduced in a controlled way by employing liquid crystal retarders, as explained in the following. The method has been first applied to estimate the depolarizing channel, namely the case of isotropic noise, with $p_1 = p_2 = p_3 = \frac{p}{3}$, where the parameter p completely specifies the channel itself, and the minimum variance (Eq. (1) for the one-dimensional case) is given by $p(1-p)$. The method has then been extended to a general Pauli channel, with independent values of the probabilities p_i .

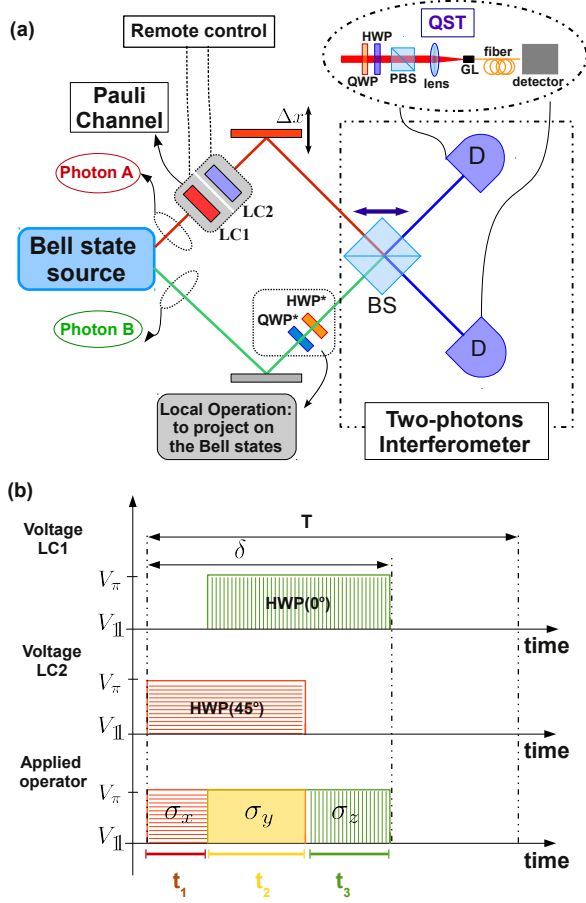


FIG. 1. a): Experimental setup. Photons A and B are spatially and temporally superimposed on a symmetric beam splitter (BS). The optical path delay Δx allows to vary the arrival time of the photons on the BS. Photons are collected by using an integrated system, composed by a GRIN lens (GL) and a single mode fiber, and then detected by single photon counters. The same setup allows to perform the Ancillary Assisted Quantum Process Tomography (AAQPT) after removing the BS. Quantum State Tomography (QST) [18] on the output state is performed by using quarter-waveplates (QWPs), half-waveplates (HWPs) and polarizing beam splitters (PBSs). b): Scheme of the implemented Pauli channel. t_1, t_2, t_3 represent the time intervals of σ_x, σ_y or σ_z activation. Both t_1, t_2, t_3 and the repetition time T can be varied by a remote control.

In order to experimentally implement the proposed optimal noise estimation protocol, we have exploited the setup shown in Fig. 1a). Precisely, a two-photon entangled source [10] generates the two-qubit singlet state $|\psi^-\rangle = \frac{1}{\sqrt{2}}(|HV\rangle_{AB} - |VH\rangle_{AB})$, where two qubits are encoded in the polarization degree of freedom, with H (V) referring to the horizontal (vertical) polarization of photons A and B.

The Pauli Channel.— Different techniques have been exploited to experimentally implement a depolarizing channel (DC) acting on a single qubit state [11–14]. In our setup the single qubit noisy channel is operating only on one of the two entangled particles (i.e. photon A). The general Pauli channel (PC) consists of a sequence of liquid crystal retarders (LC1

and LC2) in the path of photon A. The LCs act as phase retarders, with the relative phase between the ordinary and extraordinary radiation components depending on the applied voltage V . Precisely, V_π and V_\parallel (Fig. 1b) correspond to the case of LCs operating as half-waveplate (HWP) and as the identity operator, respectively. The LC1 and LC2 optical axes are set at 0° and 45° with respect to the V-polarization. Then, when the voltage V_π is applied, the LC1 (LC2) acts as a σ_z (σ_x) on the single qubit. We were able to switch between V_\parallel and V_π in a controlled way and independently for both LC1 and LC2. The simultaneous application of V_π on both LC1 and LC2 corresponds to the σ_y operation. We could also adjust the temporal delay between the intervals in which the V_π voltage is applied to the two retarders. A general PC was generated by varying the four time intervals t_1, t_2, t_3 and T which characterize the channel. Here t_1, t_2, t_3 are respectively the activation time of the operators σ_x, σ_y or σ_z and T is the period of the LCs activation cycle, as shown in Fig. 1b). The intervals t_i are related to the probabilities p_i ($i = 1, 2, 3$), introduced in Eq. (2), by the following expression: $p_i = \frac{t_i}{T}$. The probability p_0 of the identity operator is given by $p_0 = 1 - \frac{\delta}{T}$ (with $\delta = t_1 + t_2 + t_3$)

Experimental implementation of the protocol for the depolarizing channel.— The condition $t_1 = t_2 = t_3$ corresponds to the depolarizing channel, with the three Pauli operators acting on the single qubit with the same probability $p = \frac{\delta}{T} = \frac{t_1 + t_2 + t_3}{T}$. By implementing the optimal protocol it was possible to estimate the value of p corresponding to the introduced degree of noise. This parameter was changed by setting the times t_i and varying the period T .

The optimal protocol was realized by using the Bell state $|\psi^-\rangle$, as mentioned above. The DC was activated on photon A and the projective measurements $\{|\psi^-\rangle\langle\psi^-|, \mathbb{I} - |\psi^-\rangle\langle\psi^-|\}$ were performed for several noise degrees. Since the identity \mathbb{I} may be expressed as the sum of the four Bell state density matrices, the measure $\mathbb{I} - |\psi^-\rangle\langle\psi^-|$ was realized by projecting the output state on the other three Bell states.

The protocol was implemented by the interferometric setup shown in Fig. 1a). We show in the inset in Fig. 2a) the measured dip (peak) of the coincidence counts for the state $|\phi^-\rangle$ ($|\psi^-\rangle$) entering the BS in absence of noise. A half-waveplate (HWP*) and a quarter-waveplate (QWP*) (Fig. 1a) were used to project the noisy state on the other Bell states. For each noise degree, the probabilities associated to the measurement of each Bell state are related to the interference visibility measured by the interferometer.

In Fig. 2a) we report the experimental values p_i corresponding to the three Bell states $|\phi^+\rangle, |\phi^-\rangle, |\psi^+\rangle$ measured for different values of T . They are in good agreement with the expected theoretical behaviour.

Note that, in absence of noise (i.e. $\frac{1}{T} = 0$), the probabilities associated to $|\phi^+\rangle, |\phi^-\rangle, |\psi^+\rangle$ are lower than 2.5%, demonstrating that the state $|\psi^-\rangle$ was correctly generated. The higher the noise, the lower the $|\psi^-\rangle$ contribution which is only around 5% for $T = \delta$ (i.e. when the identity operator no longer acts on the qubit).

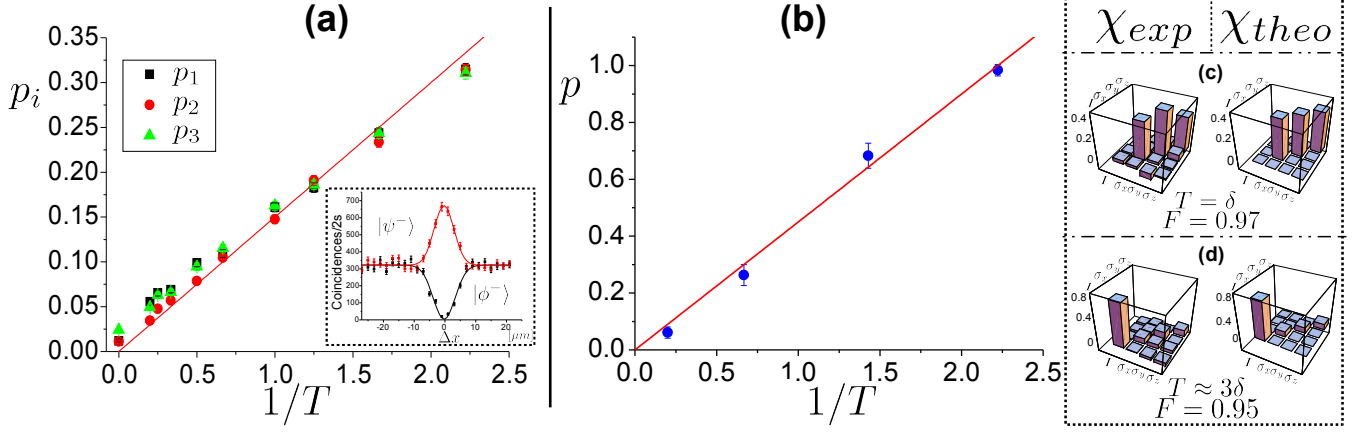


FIG. 2. a): Experimental probabilities of Bell states $|\phi^+\rangle$ (red dots), $|\phi^-\rangle$ (black squares), $|\psi^+\rangle$ (green triangles) vs. $\frac{1}{T}$. Continuous red line corresponds to the theoretical behavior. Error bars are obtained by propagating the poissonian uncertainty associated to the coincidence counts. Inset: dip (peak) of the measured coincidence counts as a function of the optical path delay for a state $|\phi^-\rangle$ ($|\psi^-\rangle$) entering the BS. b): Experimental probabilities associated to the experimental matrix χ vs $\frac{1}{T}$. Values of p are obtained by maximizing the fidelity F between theoretical and experimental matrix χ . Error bars are calculated by considering the poissonian uncertainty associated to the coincidence counts, and simulating different matrices of the process, obtaining, in this way, different values of p . c-d): Experimental (left side) and theoretical (right side) matrices χ for $T = \delta$ and $T \approx 3\delta$.

Ancillary Assisted Quantum Process Tomography.- The experimental results, just discussed for the optimal estimation of the depolarizing channel, have been compared with the probability values of p which can be obtained by exploiting the Ancillary Assisted Quantum Process Tomography (AAQPT) [13, 15–17]. The action of a generic channel operating on a single qubit can be written as $\mathcal{E}[\rho] = \sum_{i,j=0}^3 \chi_{ij} \sigma_i \rho \sigma_j$, where the matrix χ_{ij} characterizes completely the process.

AAQPT is based on the following procedure: i) prepare a two-qubit maximally entangled state; ii) send one of the two entangled qubits through the channel \mathcal{E} ; iii) reconstruct the output two-qubit state by Quantum State Tomography (QST) [18] and obtain, in this way, the matrix χ_{ij} from the two-qubit output density matrix. For a DC, the matrix χ_{ij} is expressed as [4]:

$$\chi_p^{Theo} = \begin{pmatrix} (1-p) & 0 & 0 & 0 \\ 0 & \frac{p}{3} & 0 & 0 \\ 0 & 0 & \frac{p}{3} & 0 \\ 0 & 0 & 0 & \frac{p}{3} \end{pmatrix} \quad (4)$$

We implemented the AAQPT algorithm by injecting the state $|\psi^-\rangle$ into the DC and reconstructed by QST the density matrices of the input and output states for several noise degrees [see Fig. 1a)]. We obtained the experimental matrix χ_{exp} for different values of T and, for each value of T , we found the parameter p maximizing the fidelity between the experimental χ_{exp} and the theoretical χ_p^{Theo} process matrices. The experimental results are shown in Fig. 2b). Also in this case the theoretical behaviour is fully satisfied. However, comparing these results with those obtained by the optimal protocol, we observe that the latter leads to the same results with a much lower number of measurements. Moreover, by adopting our experimental setup we were able to demonstrate that the value

of p and the DC action do not depend on the input state. In fact the AAQPT was realized with all the four Bell states entering the DC, obtaining the same results of those shown in fig. 2(b).

It is worth noting that, even if the AAQPT gives a more complete information on the process compared to the implemented optimal protocol, the latter allows to achieve a more accurate value of p . Fig. 3a) shows that, for the optimal protocol, the measured standard deviation reaches the lower bound given by $\sqrt{p(1-p)/N}$ (i.e. the square root of Eq. (1) for the one-dimensional case), where N is the dimension of the sample used to evaluate p . AAQPT standard deviations are shown in Fig. 3b). They have been calculated by a simulation based on the poissonian uncertainty associated to the coincidence counts. A hundred different matrices of the process have been simulated and the corresponding values of p have been considered in order to calculate the standard deviations. The lower optimal bound represented by the black curve is below the experimental data, demonstrating then the AAQPT is far away from the optimal estimation protocol presented in this work.

The experimental values of Fig. 3b) correspond to a sample of ~ 1600 coincidences per second. It can be evaluated that a number of 150000 coincidences per second, which is nearly two orders of magnitude larger, is needed to approach the standard deviation value of Fig. 3a).

Experimental implementation of the Pauli Channel (Anisotropic Noise).- The same experimental setup was used to implement a general Pauli channel. This can be easily achieved for different values of t_1 , t_2 and t_3 (i.e. $t_1 \neq t_2 \neq t_3$). In these measurements we set $p_0 = 0$ (corresponding to $T = \delta$) in order to investigate only the “nontrivial” action of the channel. In fact by setting $T > \delta$, the action of the

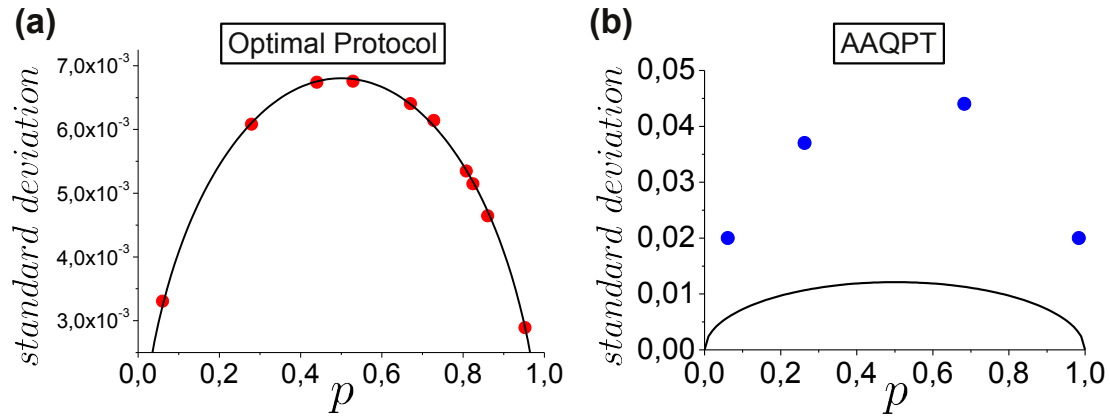


FIG. 3. a): Experimental values of the standard deviations for the optimal protocol obtained by propagating the poissonian uncertainty associated to the coincidence counts. The solid line represents the expected theoretical behaviour. b): Values of the standard deviations for the AAQPT. These have been calculated by a simulation based on the poissonian uncertainty associated to the coincidence counts. The solid line represents the optimal bound.

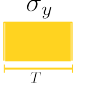
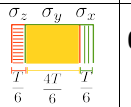
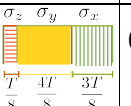
Processes applied to the input state $ \psi^-\rangle$	p_0	p_1	p_2	p_3
a) Identity	0.939 ± 0.006	0.015 ± 0.003	0.013 ± 0.003	0.033 ± 0.004
b) 	0.037 ± 0.005	0.055 ± 0.006	0.898 ± 0.008	0.010 ± 0.003
c) 	0.040 ± 0.005	0.20 ± 0.01	0.56 ± 0.01	0.20 ± 0.01
d) 	0.038 ± 0.004	0.31 ± 0.01	0.50 ± 0.01	0.154 ± 0.008

FIG. 4. Experimental probabilities of measuring the four Bell states obtained for four different cases of anisotropic noise. In the measurements shown in b), c) and d), $T = \delta$ corresponds to a complete noisy channel (i.e. $p_0 = 0$), and the input state is always $|\psi^-\rangle$. For each process, the first column shows the relative weights between the Pauli operators acting in the channel. From these values it is possible to calculate the theoretical ones. For instance, let us consider the process d) where the σ_z , σ_y and σ_x act respectively for $\frac{T}{8}$, $\frac{4T}{8}$ and $\frac{3T}{8}$. The expected values of p_i are, for this process, $p_0 = 0$, $p_1 = \frac{3}{8}$, $p_2 = \frac{4}{8}$ and $p_3 = \frac{1}{8}$. The slight disagreement between the expected theoretical values and the experimental measured ones are mainly due to the finite rise and decay times of the electrical signal driving the LC devices. a) *Identity*: only $|\psi^-\rangle$ is detected. b) σ_y : $|\psi^-\rangle$ is mapped into $|\phi^-\rangle$. c) *Partially anisotropic DC*: σ_x and σ_z operate for the same time interval, the probabilities of measuring the states $|\psi^+\rangle$ and $|\phi^+\rangle$ are equal. d) *Totally anisotropic DC*: each Pauli operator operates for a different time interval.

identity operator can be easily added to the channel (i.e. $p_0 \neq 0$). However, in this case, we demonstrate that our experimental setup allows to act separately on the three

parameters p_1, p_2, p_3 . Different configurations of the noisy channel were investigated by implementing the optimal noise protocol estimation for each configuration. A summary of four relevant experimental results, corresponding to different probabilities associated to the Bell states, are given in Fig.4.

We have implemented the protocol by using always the same input state and projecting it on the four Bell state basis. It is worth noting that this is totally equivalent to enter the DC with the four Bell states and to project them into the $|\psi^-\rangle$ state.

Conclusion.- An optimal protocol allowing the most efficient estimation of a noisy Pauli channel has been experimentally implemented in this work. The action of the noisy channel was introduced on one qubit of a maximally entangled pair in a controlled way. The efficiency of this method has been compared to the one achieved by quantum process tomography, demonstrating that the optimal protocol allows to achieve the theoretical lower bound for the errors and to perform the estimate of the noisy channel with a lower number of measurements. This method can be profitably applied when some knowledge on the noise process is available and can be successfully implemented in quantum-enhanced technologies involving the management of decoherence.

This work was supported by EU-Projects CHISTERA-QUASAR and CORNER, and by the FARI project 2010 of Sapienza Università di Roma.

-
- [1] J. I. Cirac *et al.*, Phys. Rev. A **59**, 4249 (1999).
 - [2] V. Giovannetti, S. Lloyd, and L. Maccone, Science **306**, 1330 (2004).
 - [3] V. Giovannetti, S. Lloyd, and L. Maccone, Phys. Rev. Lett. **96**, 010401 (2006).
 - [4] M. A. Nielsen and I. L. Chuang, *Quantum Computation and Quantum Information* (Cambridge University Press, Cam-

- bridge, England, 2000).
- [5] I. Bongioanni *et al.*, Phys. Rev. A **82**, 042307 (2010).
 - [6] J. L. O'Brien *et al.*, Phys. Rev. Lett. **93**, 080502 (2004).
 - [7] A. Fujiwara, Phys. Rev. A **63**, 042304 (2001).
 - [8] A. Fujiwara and H. Imai, J. Phys. A **36**, 8093 (2003).
 - [9] A. S. Holevo, *Probabilistic and Statistical Aspects of Quantum Theory*, (Amsterdam: North-Holland, 1982).
 - [10] C. Cinelli *et al.*, Phys.Rev.A **70**, 022321 (2004).
 - [11] Jin-Shi Xu *et al.*, Phys.Rev.Lett. **103**,240502 (2009).
 - [12] M. Ricci *et al.*, Phys. Rev. Lett. **93**, 170501 (2004).
 - [13] M. Karpinski, *et al.*, JOSA B **25**, 668 (2008).
 - [14] A. Shaham and H. S. Eisenberg, Phys.Rev.A **83**, 022303 (2011).
 - [15] G. M. D'Ariano and P. Lo Presti, Phys. Rev. Lett. **86**, 4195 (2001).
 - [16] M. Mohseni *et al.*, Phys. Rev. A **77**,032322 (2008).
 - [17] J. B. Altepeter, *et al.*, Phys. Rev. Lett. **90**, 193601 (2003).
 - [18] D. F. V. James *et al.*, Phys.Rev.A **64**,052312 (2001).